Polyp Segmentation Method in Colonoscopy Videos by means of MSA-DOVA Energy Maps Calculation

Jorge Bernal, Joan Manel Núñez, F. Javier Sánchez, and Fernando Vilariño

Computer Vision Centre and Computer Science Department, Campus Universitat Autònoma de Barcelona, 08193 Bellaterra, Barcelona, Spain
{jbernal,jmnunez,javier,fernando}@cvc.uab.cat
http://www.cvc.uab.es

Abstract. In this paper we present a novel polyp region segmentation method for colonoscopy videos. Our method uses valley information associated to polyp boundaries in order to provide an initial segmentation. This first segmentation is refined to eliminate boundary discontinuities caused by image artifacts or other elements of the scene. Experimental results over a publicly annotated database show that our method outperforms both general and specific segmentation methods by providing more accurate regions rich in polyp content. We also prove how image preprocessing is needed to improve final polyp region segmentation.

Keywords: Image Segmentation, Polyps, Colonoscopy, Valley Information, Energy Maps

1 Introduction

Colon cancer is nowadays the fourth most common cause of cancer death worldwide and its survival rate depends on the stage it is detected on, hence the necessity of an early colon screening [1]. Colonoscopy is currently the gold standard for colon screening although it has some drawbacks being the most relevant the miss-rate, which has been reported to be as high as 6% [2].

Combined forces between physicians and computer scientists have been coupled into a field of research referred as intelligent systems [3] which for the case of colonoscopy may be used for assisting in the diagnosis or by providing automatic quality assessment metrics [4]. Another possibility could be the development of follow-up to track a lesion over different explorations over the same patient.

Related with this last potential application, we present in this paper our Segmentation from Depth of Valley Accumulation (DOVA) Energy Maps Calculation (SDEM) algorithm for polyp segmentation in colonoscopy images. We work under the assumption that a faithful segmentation of the polyp region along with a exhaustive description of the polyp region could be potentially used to characterize polyps and will allow a posterior tracking the lesion.

Our method is built on a previously published model of appearance for polyps, which described polyp boundaries in terms of valley information [5]. This

valley information is used to generate energy maps which guide polyp localization methods [6]. Our segmentation method has been developed by considering the way the mentioned energy maps are calculated. We assess the performance of our method by comparing it with general and specific segmentation methods over a publicly annotated database.

After this introduction, we present in Section 2 related work on image segmentation, including polyp segmentation methods. We explain our segmentation method in Section 3. The experimental setup is introduced in Section 4. Experimental results are exposed in Section 5. We close this paper with the conclusions and future work in Section 6.

2 Related Work

Image segmentation in computer vision is defined as the process in which an image is divided into multiple segments -sets of pixels-. Segmentation is performed in order to simplify how an image is represented making it easier to analyze. The partitioning of the image can be based on different features, such as intensity, color or texture, and may not be unique.

Polyp segmentation methods in colonoscopy videos have been mainly applied for CT colonoscopy images [7] or chromoendoscopy [8]. Some simple segmentation methods have also been applied, although they are prone to be affected by noise and other image artifacts -specular highlights, image blurring- [9].

In this paper we will compare the performance of our method against other computer vision methods used in polyp segmentation [5], such as:

- Normalized Cuts (NCuts): The *normalized cuts* method [10] is a graph theoretic approach for solving the perceptual grouping problem in vision in which every set of points lying in the feature space is represented as a weighted, undirected graph. Segmentation is performed by disconnecting edges with small weights.
- Turbo pixels (TurPix): this algorithm [11] starts by computing a dense over segmentation of an image by means of a geometric-flow-based algorithm. This segmentation respects local image boundaries while limiting under segmentation by using a compactness constraint. Regions are refined by using criteria such as size uniformity, connectivity or compactness.
- Watershed with markers (WSM): watershed segmentation [5] considers a grayscale image as a topographic surface and achieves the segmentation by a process of "filling" of catchment basins from local minimums. Providing markers helps the algorithm to define the catchment basins that must be considered in the process of segmentation [12].
- Depth of Valleys (DoV)-based Region Merging Segmentation [5] (DV-RMS): this method assumes polyp boundaries to be described in terms of valley information. The method starts from a first rough segmentation of the input image obtained by means of watershed. The segmented regions are merged using different criteria such as boundary strength and region content.

Our novel Segmentation from Energy Maps -SDEM- algorithm is based on the characterization of polyp boundaries in terms of valley information. SDEM also considers how MSA-DOVA energy maps integrate this valley information o provide an initial segmentation of the polyp.

3 Methodology

We present here our polyp segmentation method preceded by a summary on MSA-DOVA energy maps creation which are used by our algorithm.

3.1 Generation of MSA-DOVA energy maps

MSA-DOVA energy maps are based on a model of appearance for polyps which was firstly described in [5]. This model combined information on how colonoscopy frames are acquired with the appearance of polyps in those colonoscopy frames. The model of appearance for polyps describes polyp boundaries by means of valley information. As show in [6], polyps are not the only elements of the endoluminal scene which convey valley information; image preprocessing should be applied to mitigate the contribution of these other elements such as blood vessels or specular highlights.

The following step in MSA-DOVA energy maps calculation is the obtention of the necessary valley information. Depth of Valleys image (DV) is calculated as a pixel-wise multiplication between the output of a valley detector (V) and the morphological gradient (MG):

$$DV = V(\sigma_d, \sigma_i) \cdot MG; \tag{1}$$

where V stands for the output of a valley detector [5] and MG for the morphological gradient. Morphological gradient is used to add key information about how deep is the valley in the image.

The final step consists of the calculation of MSA-DOVA energy maps, which are based on the assumption that a pixel inside a polyp should be surrounded by valleys in several directions. The calculation of these maps is based on the use of a ring of radial sectors which accumulate for each sector the maximum of DV image that falls within it. MSA-DOVA offered an improvement over sum-based accumulation as presented in [5], using a median operator to calculate the final accumulation value. MSA-DOVA accumulation value is calculated as follows:

$$MaxL(\boldsymbol{x}, \alpha) = \max_{r}\{DV(x + r * (\cos(\alpha), \sin(\alpha)))\}, \quad r \in [R_{min}, R_{max}] \tag{2}$$

$$Acc(\boldsymbol{x}) = \operatorname*{Med}_{\alpha}(MaxL(\boldsymbol{x}, \alpha)) \tag{3}$$

where R_{min} and R_{max} correspond respectively to the minimum and maximum radius of the ring of sectors and $\alpha \in [0..2\pi]$. An example of the output of MSA-DOVA energy maps is shown in Figure 1(b), where we can observe how high energy regions of the accumulation map correspond with the polyp.

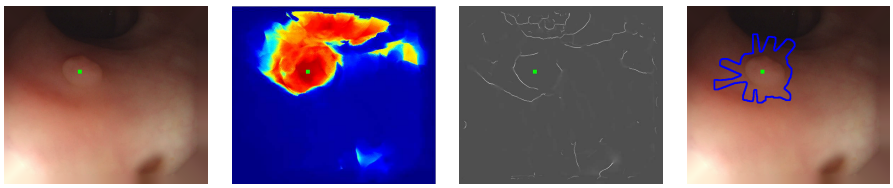

(a) (b) (c) (d)

Fig. 1. Examples of polyp segmentation from the output of an energy map: (a) Original images; (b) MSA-DOVA energy map; (c) *DV* image, and (d) Initial segmentation obtained by joining the position of the pixels that contributed to the maximum of MSA-DOVA accumulation image. Maximum of MSA-DOVA energy map is marked as a green square.

3.2 Polyp Segmentation from MSA-DOVA Energy Maps

Our polyp segmentation method -SDEM- uses information from both *DV* image and how MSA-DOVA energy maps are calculated. Our method requires that maximum of MSA-DOVA maps falls within the polyp and in this case we can obtain a first segmentation of the polyp by joining the position of the pixels that contributed to this maximum -Figures 1(b) and 1(c)-.

This first segmentation may present irregularities due to several reasons such as having an incomplete boundary in terms of valley information -see Figure 1(c)- or presence of spurious valleys from other structures in the scene. These irregularities make positions of maximum of *DV* image for adjacent sectors being not close one to another -Figure 2(a)- .

Our objective is to eliminate the irregularities in order to have a continuous and locally circular boundary -typically associated to polyps- as the contour of the final segmentation. Our method locally explores distances from maxima under each sector to the maximum of accumulation -c^{max}- to detect those positions which are far from the circumference which represents the median of the distances from each maximum to the accumulation center -Figure 2(b)-. We use the median distance as a way to correct irregular positions in favor to the most common distance value within a given neighborhood of positions. In this case the use of other options such as mean value are not suitable as the contribution of irregular positions is still taken into account for the calculation. The positions of the pixels source of irregularities are corrected to have similar distances to -c^max-. SDEM consists of the following steps:

1. Calculation of the position of the maximum of MSA-DOVA energy map as $\boldsymbol{c}^{max} \in image \mid \forall \boldsymbol{q} \in image, MSA{-}DOVA(\boldsymbol{c}^{max}) \geq MSA{-}DOVA(\boldsymbol{q}^{max})$.
2. Definition of a ring of ns radial sectors centred in $\boldsymbol{c}^{max}$.
3. Calculation of the position of the maximum of *DV* image under each sector S_i of the ring as $\boldsymbol{p}_i^{max} \in S_i \mid \forall k \in S_i, DV(\boldsymbol{c}_i^{max}) \geq DV(q)$, with $i \in [1, ns]$.
4. Conversion of the position of the maximum of *DV* under each sector $\boldsymbol{p}_i^{max}$ to polar domain $\boldsymbol{\rho}_i^{max} = [r_i^{max}, \theta_i^{max}]$, where r stands for the radial coordinate and θ for the angular coordinate.

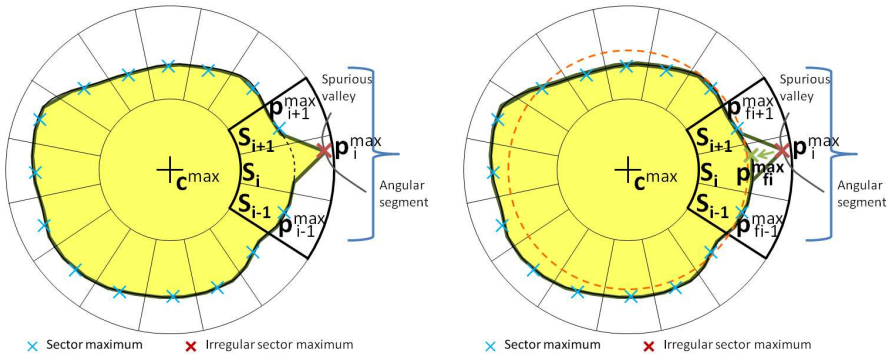

Fig. 2. Graphical explanation of SDEM algorithm. We label maximum under each sector as blue crosses. For the case of the irregularity, we label the original position as a red cross whereas the corrected position is marked as a green cross. A circumference showing the median of distances to center is depicted as discontinuous green line.

5. Definition of an angular segment of size $2ws$ centred on S_i -Figure 2(a)-.
6. Calculation of the new radial coordinate by means of the median of the r_j values of the angular segment $r_{fi}^{max} = median(r_j^{max}), j \in [i - ws, i + ws]$.
7. Definition of the new polar coordinates of as $\boldsymbol{\rho}_{fi}^{max} = [r_{fi}^{max}, \theta_i^{max}]$
8. Revert the conversion to cartesian coordinates. The final position of maximum under S_i is referred as $\boldsymbol{p}_{fi}^{max}$ -Figure 2(b)-.

SDEM algorithm has only one proper parameter ws which is the size of the angular segment. MSA-DOVA parameters -minimum radii -*radmin*-, maximum radii -*radmax*- and *ns*- are set to the values published in the original paper ($radmin = 25$,$radmax = 135$ and $ns = 180$). To close with the explanation, we present a qualitative example of segmentation refinement in Figure 3.

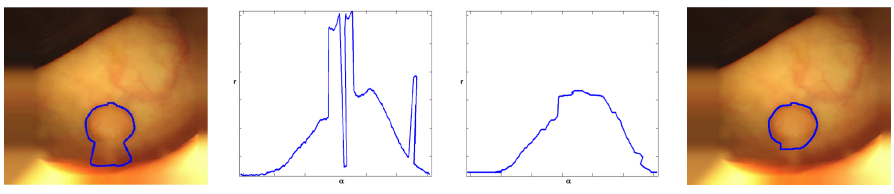

Fig. 3. Softening of boundaries by median filtering in polar space: (a) Preprocessed image with initial segmentation; (b) Polar representation of the initial segmentation; (c) Polar representation of the segmentation after median correction; (d) Preprocessed image with final segmentation.

4 Experimental Setup

Our segmentation method will be validated on the only public fully annotated database, (*CVC-ColonDB*) introduced in [5]. As in the original work, we will only use a subset of 300 frames from the main database as some sequences were discarded due to bad image quality or presence of fecal content.

AAC, DICE [9] and F_2 score metrics will be used to compare the performance of the different methods. In this case we compare at pixel-level segmentations provided by the output of the different methods with the ground truth. The metrics are defined as follows:

$$AAC = 100 \cdot \frac{TP}{TP + FP} \quad DICE = 100 \cdot \frac{TP}{TP + FN} \quad F_2 = \frac{5AAC \cdot DICE}{4AAC + DICE} \quad (4)$$

where TP, FP and FN stand for the number of True Positive, False Positive and False Negative pixels, respectively.

We compare our method with general segmentation methods -NCuts and TurPix- and valley information-based methods -WSM and DV-RMS- using the proposed metrics. All the methods in the comparison are used with the parameter configuration described in our previous contribution [5]. We remark that both NCuts and TurPix need to be provided with a number of target regions nr to be extracted. After performing several segmentation tests we selected $nr = 3$ as the most representative result, considering that colonoscopy images present three main regions which are: 1) lumen; 2) polyp; 3) colon wall. For all the methods we used the position of maximum of MSA-DOVA to select the final polyp region. Regarding SDEM, we set $ws = 20$ -corresponding to an angular segment of ± 40 deg- after a training state over 30 images not part of the database.

5 Experimental Results

In order to focus on segmentation, results will be analyzed only for those images in which the polyp localization succeeded. The experiments were performed using as input both the original and the preprocessed image.

We can observe in Table 1 that our proposal outperforms the rest of approaches, specially in terms of AAC. Our method provides with regions with a higher amount of polyp content while adding less non-polyp areas. This result is confirmed by F_2-score. Our method provides with a segmentation that covers almost the 70% of the polyp region -much higher than the other methods- whereas it still keeps a reasonably high performance in terms of DICE. Our proposal also improves the results achieved by our most similar competitor -WSM-: segmentation guided by energy maps leads to obtain bigger final regions closer to the actual polyp region.

Regarding the impact of image preprocessing we can also notice that our method still outperforms the rest of approaches, being our final regions are now much richer in terms of polyp content -81.22% vs. 69.32%- although slightly smaller. This can be interpreted as our regions being now more inscribed inside

	Without preprocessing			With preprocessing		
Method	AAC [%]	DICE [%]	F_2	AAC [%]	DICE [%]	F_2
NCuts	20.29	80.27	0.50	18.02	83.84	0.48
TurPix	19.40	75.56	0.47	14.75	76.30	0.41
WSM	42.89	68.36	0.61	43.68	74.40	0.65
DoV-RMS	56.87	44.93	0.47	54.13	57.46	0.56
SDEM	69.93	69.32	**0.69**	65.07	81.22	**0.77**

Table 1. Segmentation results with -160 images- and without image preprocessing -203 images-.

the polyp mask, removing more non-polyp content. Image preprocessing also has an impact in the performance of the rest of the methods, being watershed with MSA-DOVA markers the only one in which there is improvement in both precision and recall results.

Finally we present some qualitative results on polyp segmentation in Figure 4 some qualitative examples of polyp segmentation of several images before and after applying preprocessing operations.

6 Conclusions and Future Work

We have presented a novel polyp segmentation method in colonoscopy videos, which is built on a general model of appearance for polyps which describes polyp boundaries using valley information. This information is integrated to generate energy maps linked with polyp presence in the image. Our method explores the way these maps are created to develop a polyp region segmentation algorithm, considering which pixels in the image contributed to the localization of the polyp. Our algorithm is able to improve an initial segmentation by adjusting the shape of the final region discarding some contributions prone to provide irregularity.

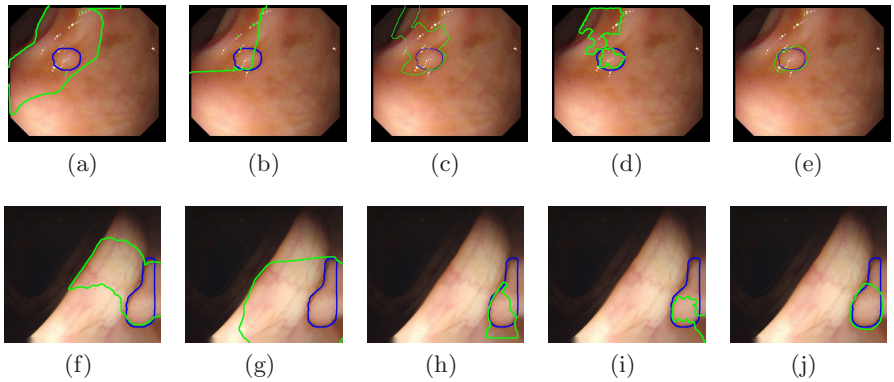

Fig. 4. Examples of polyp segmentation results: (a-f) Normalized Cuts; (b-g) Turbo Pixels; (c-h) Watershed with MSA-DOVA markers; (d-i) PR and (e-j) Our proposal. Each image shows segmentation output (green) and polyp mask (blue). Top row shows results without image preprocessing, bottom row with image preprocessing operations applied.

The results show that our method outperforms other general and specific segmentation methods in terms of AAC, DICE and F2 measure. Our experiments also confirm the necessity of image preprocessing to improve the final segmentation of the polyp.

Nevertheless our results need to be further improved if our method is to be used to potentially track polyps over different interventions. Future work should consist of addressing the impact of elements of the scene not yet covered such as folds or intestinal content. The algorithm should also be tested on a full sequence rather than on individual frames to test the validity of our hypothesis.

ACKNOWLEDGMENTS

This work was supported by a research grant from Universitat Autónoma de Barcelona 471-01- 2/2010 and by Spanish projects $TIN2009-10435$, $TIN2009-13618$ and $TIN2012-33116$.

References

[1] Tresca, A., "The Stages of Colon and Rectal Cancer," *New York Times (About.com)*, p. 1, 2010.

[2] B. Bressler, L.F. Paszat et al., "Rates of new or missed colorectal cancers after colonoscopy and their risk factors: a population-based analysis," *Gastroenterology*, vol. 132, no. 1, pp. 96–102, 2007.

[3] J. Bernal, F. Vilariño, and F. J. Sánchez, *Colonoscopy Book 1: Towards Intelligent Systems for Colonoscopy*. In-Tech, 2011.

[4] J. Oh, S. Hwang et al., "Measuring objective quality of colonoscopy," *IEE T Bio-Med Eng*, vol. 56, no. 9, pp. 2190–2196, 2009.

[5] J. Bernal, F. J. Sánchez, and F. Vilariño, "Towards automatic polyp detection with a polyp appearance model," *Pattern Recognition*, 2012.

[6] J. Bernal, F. J. Sánchez, and F. Vilariño, "Impact of image preprocessing methods on polyp localization in colonoscopy frames," in *Proceedings of the 35th IEEE EMBC*, (Osaka, Japan), (in press), July 2013.

[7] H. Wang, L.C. Li et al., "A novel colonic polyp volume segmentation method for computer tomographic colonography," in *SPIE Medical Imaging*, pp. 90352W–90352W, International Society for Optics and Photonics, 2014.

[8] M. Häfner, A. Uhl, and G. Wimmer, "A novel shape feature descriptor for the classification of polyps in hd colonoscopy," in *Medical Computer Vision. Large Data in Medical Imaging*, pp. 205–213, Springer, 2014.

[9] F. Riaz, M. Ribeiro, and M. Coimbra, "Quantitative comparison of segmentation methods for in-body images," in *Proceedings of EMBC 2009*, pp. 5785 –5788, September 2009.

[10] J. Shi and J. Malik, "Normalized cuts and image segmentation," *Pattern Analysis and Machine Intelligence, IEEE Transactions on*, vol. 22, no. 8, pp. 888–905, 2002.

[11] A. Levinshtein, A. Stere, K. Kutulakos, D. Fleet, S. Dickinson, and K. Siddiqi, "Turbopixels: Fast superpixels using geometric flows," *Pattern Analysis and Machine Intelligence, IEEE Transactions on*, vol. 31, no. 12, pp. 2290–2297, 2009.

[12] X. Zhang, F. Jia, S. Luo, G. Liu, and Q. Hu, "A marker-based watershed method for x-ray image segmentation," *Computer methods and programs in biomedicine*, 2014.